Local modifications of magnetism and structure in FePt (001) epitaxial thin films by focused ion beam: Two-dimensional perpendicular patterns

F. Albertini, L. Nasi, F. Casoli, S. Fabbrici, P. Luches et al.

Additional information on J. Appl. Phys.

Local modifications of magnetism and structure in FePt (001) epitaxial thin films by focused ion beam: Two-dimensional perpendicular patterns

F. Albertini,[1,a)] L. Nasi,[1] F. Casoli,[1] S. Fabbrici,[1] P. Luches,[2] G. C. Gazzadi,[2] A. di Bona,[2] P. Vavassori,[3] S. Valeri,[4] and S. F. Contri[4]

[1]IMEM-CNR, Parco Area delle Scienze 37/A, I-43010 Parma, Italy
[2]S3 CNR-INFM, via G. Campi 213/a, I-41100 Modena, Italy
[3]S3 CNR-INFM, via G. Campi 213/a, I-41100 Modena, Italy, Dipartimento di Fisica, Università di Ferrara, via Saragat 1, I-44100, Italy, and CIC nanoGUNE Consolider, Mikeletegi Pasealekua 56, E-20009 San Sebastian, Spain
[4]S3 CNR-INFM, via G. Campi 213/a, I-41100 Modena, Italy and Dipartimento di Fisica, Università di Modena, via G. Campi 213/a, I-41100 Modena, Italy

Focused ion beam was utilized to locally modify magnetism and structure of $L1_0$ FePt perpendicular thin films. As a first step, we have performed a magnetic, morphological, and structural study of completely irradiated FePt films with different Ga^+ doses (1×10^{13} – 4×10^{16} ions/cm²) and ion beam energy of 30 keV. For doses of 1×10^{14} ions/cm² and above a complete transition from the ordered $L1_0$ to the disordered A1 phase was found to occur, resulting in a drop of magnetic anisotropy and in the consequent moment reorientation from out-of-plane to in-plane. The lowest effective dose in disordering the structure (1×10^{14} ions/cm²) was found not to affect the film morphology. Taking advantage of these results, continuous two-dimensional (2D) patterns of perpendicular magnetic structures (250 nm dots, 1 μm dots, 1 μm-large stripes) were produced by focused ion beam without affecting the morphology. The 2D patterns were revealed by means of magnetic force microscopy, that evidenced peculiar domain structures in the case of 1 μm dots. © 2008 American Institute of Physics. [DOI: 10.1063/1.2975217]

I. INTRODUCTION

FePt $L1_0$-ordered alloy is a "natural" multilayer constituted of pure Fe and pure Pt layers. Pt sublattice, which is spin polarized by neighboring $3d$ atoms, gives a small contribution to saturation magnetization. On the other hand it plays a primary role in determining huge values of magnetocrystalline anisotropy ($>10^6$ J/m³) due to spin-orbit coupling on Pt and to a strong hybridization between Pt $5d$ and Fe $3d$ states.[1] This property makes the material very promising for a variety of advanced applications concerning hard magnetism (see Refs. 2–4 and references therein).

Recently, it has been widely studied for possible applications in magnetic recording media where the high magnetocrystalline anisotropy allows the ferromagnetic stability in particles of few nanometers, and consequently the achievement of ultrahigh density of information.[5,6] The perpendicular geometry of recording is a viable solution to postpone the superparamagnetic limit.[7,8] FePt $L1_0$ with (001) orientation represents a suitable material.[9] The perpendicular orientation of the easy axis (i.e., c-axis, the shortest) can be obtained by high-temperature epitaxial growth on suitable substrates.[10,11]

A further approach to address the superparamagnetic challenge in order to increase the information density is the realization of patterned magnetic media.[5,12] Examples are represented by single-grain-per-bit media or by discrete track recording media.[13] In order to preserve surface flatness of the medium and to avoid the detrimental effects due to the worsening of surface quality, two-dimensional (2D) magnetic patterns in continuous films obtained by ion irradiation have also been proposed.[14]

Ion irradiation has revealed to be a very flexible tool to tailor the main magnetic properties (e.g., anisotropy, coercivity, exchange interaction, Curie temperature) of thin films and multilayers, giving rise to several effects, depending on the choice of ions, doses and energies, like intermixing, modification of morphology, interface quality and strain, modification of crystallinity and chemical composition, production of vacancies and pinning centers.[15–22]

Several investigations have been performed on Co/Pt and Fe/Pt multilayers.[14,23] In this case, two main effects are produced by ion irradiation: alloying of the two elements resulting in the modification of the magnetic state (ferromagnetic/paramagnetic) and intermixing at interfaces resulting in the modification of the magnetic anisotropy (parallel/perpendicular).

Recently, some papers have also been devoted to thin films based on FePt and CoPt alloys. On the one side, ion irradiation was found to induce chemical order in FePt disordered A1 structure, triggering and controlling the ordering process at temperatures well below the standard ones.[24–26] On the other side, ion irradiation with suitable conditions was found to destroy chemical order in $L1_0$ thin films.[27–29] In particular, on FePt $L1_0$ the effects of irradiation with different ions and beam energy have been investigated in nonoriented thin films.[30]

It is worth noticing that in (001) epitaxial $L1_0$ FePt the direction and the intensity of the magnetocrystalline aniso-

---

a)Electronic mail: franca@imem.cnr.it.

tropy are very sensitive to structural order and crystallographic orientation. Therefore it appears to be the ideal candidate for the realization of smooth and continuous patterned perpendicular systems, by locally modifying the degree of structural order by ion irradiation. The aim of the present investigation is to obtain 2D patterns of perpendicular magnetic structures based on FePt (001) epitaxial thin films, by controlling coercivity and direction of magnetization (i.e., out-of-plane versus in-plane) by means of maskless Ga^+ irradiation with focused ion beam (FIB). In order to get a precise control of the properties during patterning, a detailed study of the effects of different Ga^+ doses on structure, morphology and magnetism of FePt (001) epitaxial thin films was performed.

II. EXPERIMENTAL PROCEDURES

Epitaxial $L1_0$ (001) perpendicular thin films of thickness $t = 10$ nm were grown on MgO (100) by RF sputtering by alternating the deposition of very thin Fe and Pt layers with nominal thickness of about 0.2 nm. Due to the miscibility of the two metals and the relatively high growth temperatures, the growth proceeds under conditions similar to codeposition. The chosen ratio between the individual thicknesses corresponds to a nominal atomic composition of $Fe_{53}Pt_{47}$. The growth was performed at a $T_S = 400$ °C, directly measured with a thermocouple in contact with the substrate.

The films were subsequently exposed to ion irradiation by FIB apparatus, FEI DB235M Dual Beam system, combining a Ga^+ FIB and a thermal field emission scanning electron microscope (SEM), working at coincidence on the sample with doses up to 4×10^{16} ions/cm^2. An ion energy of 30 keV and currents in the nA range were employed.

Structural characterization was done by means of x-ray diffraction in theta-2theta and grazing incidence (GiXRD) configuration, using a Thermo ARL X'tra diffractometer equipped with parabolic mirror on the Cu $K\alpha$ incident beam and a Si(Li) Peltier detector.

Auger electron spectroscopy (AES) was used to extract information on the Ga concentration in the irradiated areas. A scanning Auger system with a primary beam energy of 3 keV was used.

Morphological characterization was performed by atomic force microscopy (AFM) in tapping mode by a Dimension 3100 Scanning Probe Microscope equipped with a Nanoscope IVa controller (Veeco Instruments) and by scanning tunnel microscopy (STM) by an Omicron UHV AFM/STM (biased sample and grounded tip).

Magnetic measurements were performed at room temperature by alternating gradient force magnetometry (AGFM) in parallel and perpendicular configuration. Magneto-optical Kerr effect (MOKE) magnetometry in the longitudinal and polar configurations was also used to characterize the magnetic properties. The laser beam was focused to a spot with a diameter of about 30 μm (μMOKE). Magnetic force microscopy (MFM) in interleave mode was performed to characterize magnetic domain structure of as-deposited and patterned thin films.
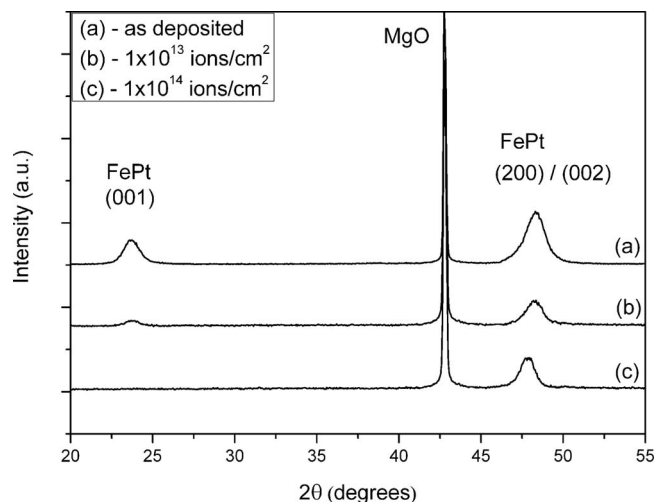
FIG. 1. XRD patterns of FePt films: as-deposited (a) and subjected to Ga^+ ions irradiation with doses 1×10^{13} (b) and 1×10^{14} (c); relative intensities between patterns are not in scale.

III. RESULTS AND DISCUSSION

A. As-deposited films

Structural measurements performed by XRD, GiXRD, and selected area electron diffraction[31] confirmed the epitaxial growth on MgO (100) of the high-anisotropy $L1_0$ phase, with a perpendicular orientation of the c-axis. The formation of the ordered $L1_0$ phase is proved by the appearance of the (001) superstructure reflection in the theta-2theta XRD plots of the as-deposited films [Fig. 1(a)].

Parallel and perpendicular magnetization loops measured by AGFM confirm the structural results, showing high values of magnetocrystalline anisotropy and high degree of perpendicular orientation (Fig. 2). However, a 5.7% parallel remanence ratio, calculated as $(M_r\| / M_S)$, is present. This point out that a small amount of disordered phase, not apparent in the XRD spectrum, is present. In order to have information on possible in-plane anisotropies in the residual phase we measured longitudinal MOKE hysteresis cycles with the magnetic field applied along different in-plane directions. The cycles on a 180° range in steps of 30° starting from one of the [100] directions are shown in Fig. 3. The measurements were performed in the longitudinal configura-
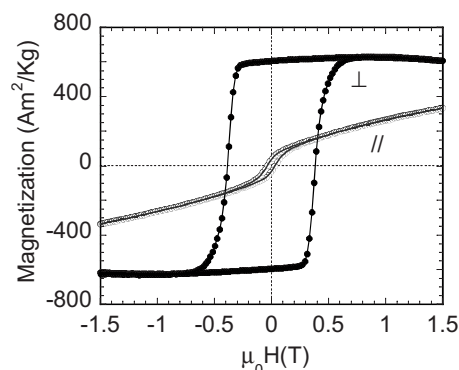
FIG. 2. Parallel (open symbols) and perpendicular (full symbols) magnetic hysteresis loops measured by alternating gradient force magnetometer at room temperature of as-deposited FePt thin film.
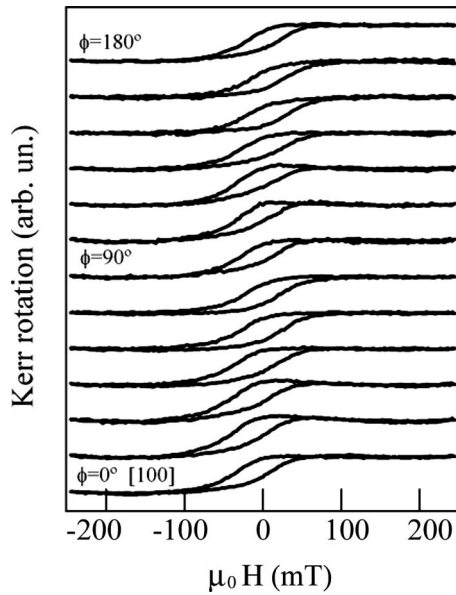
FIG. 3. Longitudinal MOKE hysteresis loops of as-deposited FePt film. The cycles were measured at room temperature with the magnetic field applied along different in-plane directions.

FIG. 4. (Color online) Morphology characterization of as-deposited FePt film. (a) 500 nm×500 nm STM image with 0.1 nA and V_{sample}=−0.5 V; (b) height profile along the marked line in (a).

tion using the modulation polarization technique. In this configuration the measured signal contains contributions arising from the magnetization component perpendicular to the plane of the film as well as from the in-plane component parallel to the applied field.[32] In order to isolate the in-plane component of the soft phase from the contributions coming from the in- and out-of-plane magnetization components of the hard phase, we subtracted from each loop a line and a parabola, respectively. No relevant differences in the shape of the cycles could be detected, indicating that the residual soft phase is isotropic in plane and it has a coercive field of approximately 300 Oe.

The effective magnetocrystalline anisotropy constant K_{eff}, calculated as $K_{eff}=H_A M_S/2$, resulted to be $\sim 1.5 \times 10^6$ J/m^3, where H_A is the anisotropy field, obtained by extrapolating the parallel loop to the perpendicular saturation magnetization, as measured by AGFM. Other important magnetic properties of perpendicular loops are the following: squareness Sq=0.9 (Sq=area of the loop in the second quadrant divided by the product $H_C 0 M_r$) and perpendicular coercivity $\mu_0 H_C$=0.38 T. The above characteristics (i.e., high anisotropy, squareness close to 1 and moderate coercivity) satisfy important requirements for perpendicular recording media.[11] They have also been exploited for the realization of the hard phase in perpendicular hard-soft exchange-coupled bilayers.[3,4,33]

The obtained characteristics are likely to be linked to the peculiar morphology obtained by using the present growth method. Accurate morphology characterization was performed by means of AFM, STM, and SEM. AFM measurements show interconnected grains with a maze-like morphology. In order to increase sensitivity and to exclude tip-convolution effects, STM measurements were also performed [Fig. 4(a)]. The good quality of the STM images definitely confirms that the grains are interconnected. The presence of regions of uncovered MgO surface between the
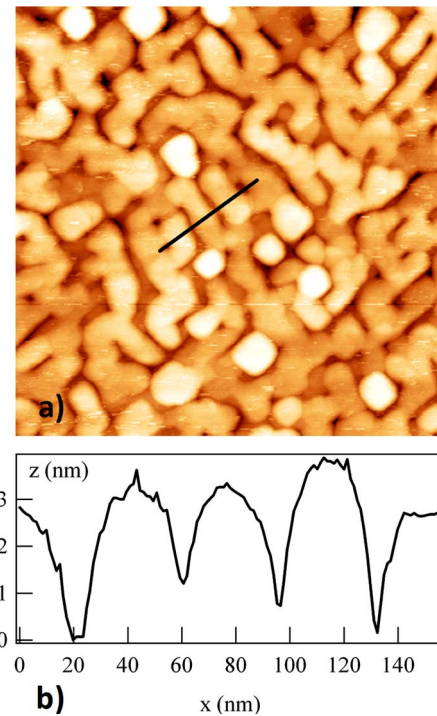
grains would in fact preclude the possibility of applying this technique. The profile plots of STM measurements for as-deposited samples show that the maximum height of the grains is approximately half the films thickness [Fig. 4(b)]. The measured roughness is 1–1.5 nm for the as-deposited film. The maze-like morphology of the films is given by interconnected square or rectangular grains with sides oriented along the FePt [110] direction and with a transversal dimension ranging from 20 to 40 nm [Fig. 4(a)].

With the present preparation method we obtained continuous films with high anisotropy. In the literature similar anisotropy values were found for noncontinuous films characterized by an island-like morphology obtained at a higher deposition temperature, and displaying much higher coercivity.[9] This fact could indicate that with our deposition technique, i.e., alternated-layer deposition by RF sputtering, it is possible to obtain higher anisotropy at lower growth temperatures.[31,34] On the other hand, a direct comparison between growth temperatures in different apparatus is quite difficult.

The high ratio between anisotropy and coercivity ε =H_A/H_C=11 and the high values of squareness have to be attributed to the continuous morphology (non-island-like). Such a morphology also allows the presence of continuous domain patterns characterized by demagnetizing factors much lower than 1.[31,35] Magnetic force microscopy measurements (Fig. 5) confirm a similar scenario. The domains are reminiscent of the maze-like pattern shown by thick platelets with perpendicular magnetization and low coercivity,[36] but show irregularities both in the domain shape and size. The Fourier analysis of the MFM image does not show one definite periodicity but different predominant values in the range 250–610 nm.
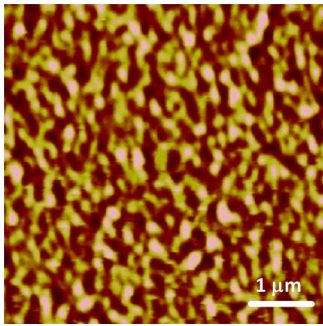
FIG. 5. (Color online) 5 μm$\times$5 μm MFM image of as-deposited FePt film.

B. Effects of Ga⁺ irradiation

The obtained FePt (001) epitaxial thin films were subsequently processed by Ga⁺ irradiation, with doses ranging from 1×10^{13} to 4×10^{16} ions/cm², to study in detail the effects of different Ga⁺ doses on structure, morphology and magnetism. TRIM simulations allowed to calculate the optimum ion energy to be used.[37] The simulations were performed for Ga⁺ ions on a 10 nm thick FePt layer changing the ion energy within the experimentally accessible range, i.e., from 5 to 30 keV. The fraction of incident ions implanted within the FePt film decreases from 100% at 5 keV to 54% at 30 keV, due to the increasing penetration range.

Therefore, in order to minimize the Ga content into the film, in the present paper we have chosen an ion beam energy of 30 keV. On the other hand, it is known that besides the dose, the energy of ions plays an important role in changing the magnetic properties of materials.[30] This point would deserve further investigations in view of possible industrial applications.

The concentration of implanted Ga⁺ ions within the film was also measured by AES on the uniformly irradiated FePt films, after removing the surface contamination by 10 min mild sputtering. The average Ga concentration was estimated to be 10% at 2×10^{16} ions/cm² and was found to fastly decrease to values around 2% at ion doses of 1×10^{16} ions/cm². Such a rapid drop of Ga concentration suggests that at the lowest doses the magnetic moment dilution due to implanted Ga⁺ ions is negligible.

TRIM simulations have also allowed to calculate the average number of displaced atoms within the FePt film to be about 2.8×10^{-1} per incoming ion per nm. The number of vacancies created in FePt corresponds to less than 1% of the number of atoms at 1×10^{14} ions/cm², where no significant amorphization effect is expected to occur. However, at a much higher dose (1.3×10^{16} ions/cm²) the concentration of vacancies is calculated to be of the same order of magnitude of the atomic density, and therefore a more relevant presence of defects is expected.

From x-ray analysis it was found that the irradiation process worsens the order extent; even the smallest dose of Ga⁺ ions makes the long-range order parameter S decrease: i.e., an irradiating dose of 1×10^{13} ions/cm² worsens the order parameter S from the initial value of 0.53 to 0.17, as calculated from the integrated intensities of the (001) and (002) peaks.[38] X-ray diffraction patterns for as grown and irradi-

TABLE I. Structural parameters measured by means of x-ray diffraction for as-deposited $L1_0$ FePt and irradiated samples. As a reference, literature reports the following bulk values as FePt cell parameters: $L1_0$ $a=3.8525(3)$ $c=3.7133(5)$. A1 cubic phase $a=3.816(5)$ (Ref. 39). The long-range order parameter S has been calculated following Cebollada *et al.* (Ref. 38).

Irradiation (ions/cm²)	S	$d(001)$ (Å)	$2\times d(002)$ (Å)
0	0.53(2)	3.742(7)	3.759(7)
1×10^{13}	0.17(2)	3.745(7)	3.761(7)
1×10^{14}			3.798(7)
5×10^{14}			3.804(7)
1×10^{15}			3.804(7)
2×10^{15}			3.797(7)
3×10^{15}			3.806(7)

ated samples with doses of 1×10^{13} and 1×10^{14} are reported in Fig. 1, while the structural parameters of films irradiated with different doses are shown in Table I.

The lowest effective dose for which the complete disordering from $L1_0$ to A1 phase takes place was found to be 1×10^{14} ions/cm²: The FePt (001) superstructure reflection completely disappears [Fig. 1(c)] and the lattice parameter assumes a value typical of the a-axis of the disordered A1 phase.[39] Further irradiation does not bring any change in the structural parameters (Table I).

The magnetization loops measured by AGFM in parallel and perpendicular configuration for the film irradiated with the above dose (1×10^{14} ions/cm²) are reported in Fig. 6. The disordering from tetragonal $L1_0$ to cubic A1 eliminates the perpendicular magnetocrystalline anisotropy that arises from the ordered structure, made of pure Fe and Pt layers. As a consequence, the perpendicular coercivity drops from $\mu_0H_C=0.38$ T to $\mu_0H_C=0.016$ T. It is also worth noticing that the drop of perpendicular anisotropy produces a spin reorientation transition corresponding to a change of easy-magnetization direction from perpendicular to in-plane. Concomitantly, MFM signal drops to zero. In fact it is sensitive to the perpendicular component of the force due to stray fields gradients exerted on a perpendicularly magnetized tip. The saturation field in the perpendicular loop corresponds to the shape-anisotropy field. Its value is consistent with the
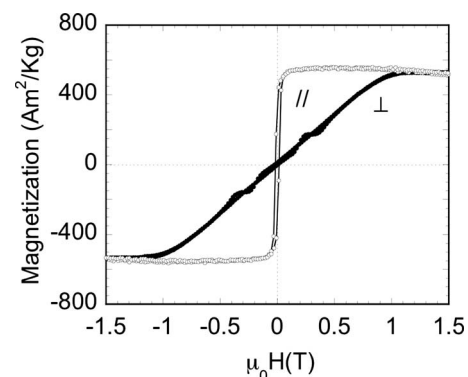
FIG. 6. Parallel (open symbols) and perpendicular (full symbols) magnetic hysteresis loops measured by alternating gradient force magnetometer at room temperature of irradiated FePt film (dose=1×10^{14} ions/cm²).
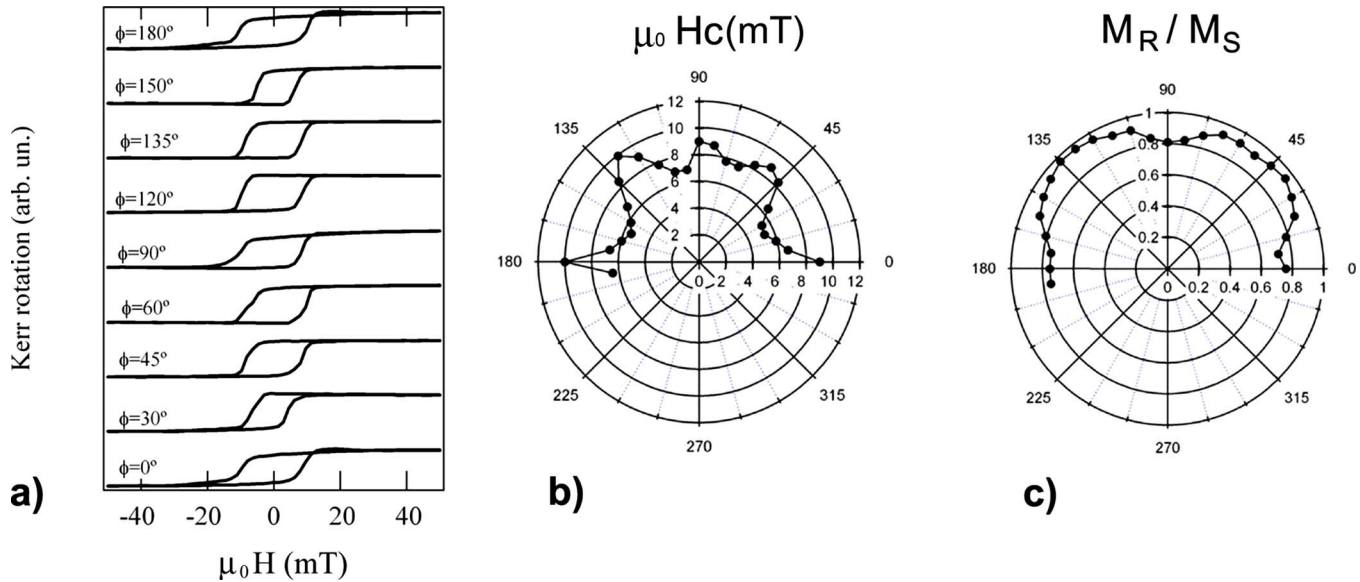
FIG. 7. (Color online) Longitudinal MOKE hysteresis measurements of the irradiated FePt film (dose=1×10^{14} ions/cm^2) at room temperature with the magnetic field applied along different in-plane directions: (a) magnetization hysteresis loops; (b) polar plot of magnetic coercivity as a function of the applied field direction; (c) polar plot of the normalized magnetic remanence (M_R/M_S) as a function of the applied field direction.

choice of a demagnetizing factor $N \sim 1$ (infinite plate). The same behavior was found to occur also for higher doses.

Hysteresis loops of irradiated films with a dose of 1×10^{14} ions/cm^2 were also measured by Kerr magnetometry in s polarization with the field applied along different in-plane directions on a 187.5° range in steps of 7.5° starting from the [100] one. A selection of the measured loops is shown in Fig. 7(a). The magnetic coercivity [Fig. 7(b)] shows maximum values $\mu_0 H_C \sim 0.1$ T along the $\langle 100 \rangle$ and $\langle 110 \rangle$ directions and minimum values in between. The M_R/M_S value instead shows minimum values along the $\langle 100 \rangle$ directions and maxima (~ 0.97) along the $\langle 110 \rangle$ directions, suggesting the presence of a magnetization easy axis along the $\langle 110 \rangle$ directions. In this case, differently from the easy-plane residual phase in as-deposited film, the soft phase displays an in-plane preferential magnetization orientation, due to the high degree of crystalline (100) orientation of A1 phase on MgO (100).

The effect of ion irradiation on thin film morphology was also investigated. In particular, at the lowest effective

dose for a complete disordering of $L1_0$ structure (1×10^{14} ions/cm^2), the morphology was found not to be affected by ion irradiation. In Fig. 8 we report a SEM picture of a partially irradiated sample with 1×10^{14} ions/cm^2, showing a perfect continuity of the maze-like granular structure, passing through the boundary between irradiated and nonirradiated (left-hand side) zones. No noticeable effect on morphology was found to occur in irradiated samples with doses up to 3×10^{15} ions/cm^2. In order to have a better insight into the sputtering effects on the surface morphology, small areas of 100 μm $\times$ 100 μm were irradiated with doses from 8×10^{15} up to 4×10^{16} ions/cm^2 and studied by AFM. In Fig. 9 images for selected doses have been reported. A small enlargement of grains, accompanied by an increase of the surface roughness from 0.5 nm to 0.9 nm is the main effect of the Ga$^+$ irradiation with doses in the range 8×10^{15}–1×10^{16} ions/cm^2. The effects of surface erosion become pronounced after irradiation with 2×10^{16} and 4×10^{16} ions/cm^2: At these doses, the original maze-like morphology is completely destroyed, leaving a dot-like pattern with roughness of about 1.5 nm, as shown in Fig. 9(c).

C. Patterned films

By using the lowest effective dose (1×10^{14} ions/cm^2) two-dimensional continuous patterns were fabricated. In particular, three patterns composed of hard magnetic $L1_0$ perpendicular and soft A1 parallel structures were produced.
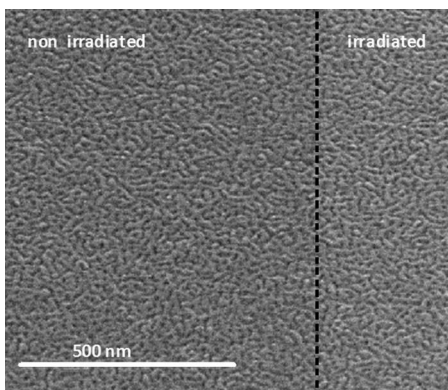
FIG. 8. *In-situ* high-resolution SEM image of a partially irradiated FePt film (dose=1×10^{14} ions/cm^2).
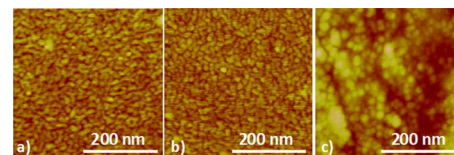
FIG. 9. (Color online) Tapping-mode AFM images of FePt films irradiated with doses: (a) 8×10^{15}, (b) 1×10^{16}, and (c) 4×10^{16} ions/cm^2.
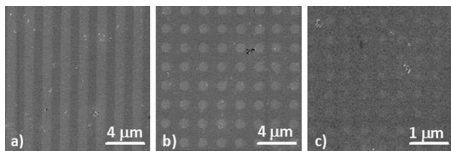
FIG. 10. SEM images of the patterned arrays obtained by irradiating selected regions of FePt film with a dose of 1×10^{14} ions/cm^2: (a) 1 μm stripes, (b) 1 μm-diameter dots, and (c) 250 nm-diameter dots.

The first pattern was made by alternating irradiated (soft) and nonirradiated (hard) stripes with lateral size of 1 μm. The others consisted of nonirradiated dots surrounded by an irradiated matrix. Dots have 1 μm and 250 nm diameters (D) and are arranged in square array with period $d=2D$.

In Fig. 10 *in-situ* high-resolution images of the patterned arrays obtained by SEM are reported. It is worth noticing that the morphology of the film shows the same maze-like interconnected grains, with no evidence of swelling effects. This is in agreement with results on FIB-irradiated metals, where swelling is not typically observed; moreover, the empty space in between the grains would probably allow to accommodate a volume increase in the film by lateral expansion. Due to the preservation of surface quality after irradiation, the AFM measurements in standard tapping mode are practically insensitive to ion irradiation. On the other hand, MFM, performed with a tip magnetized perpendicularly to the film is sensitive to the perpendicular stray field gradients emanating from the sample and consequently to the magnetic patterns.[40] In fact they present hard and soft zones corresponding respectively to perpendicular and parallel magnetization directions. MFM large-scale images are reported in Fig. 11. The signal in the irradiated regions is due to background noise.

FIG. 11. (Color online) Large-area MFM images of the 2D patterned FePt films obtained by ion irradiation (dose=1×10^{14} ions/cm^2) showing contrast from hard/soft regions: (a) 1 μm stripes, (b) 1 μm-diameter dots array. The signal in the dark-irradiated regions is due to background noise.
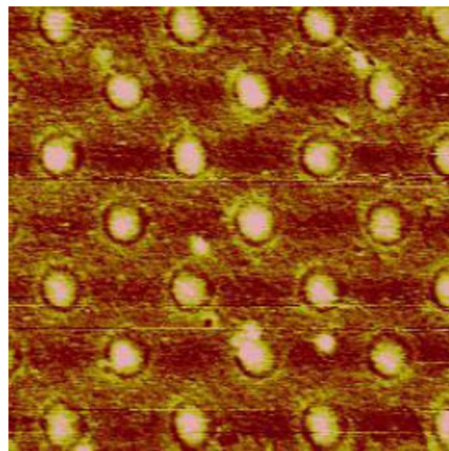
FIG. 12. (Color online) MFM image of the 2D patterned FePt films of 1 μm-diameter nonirradiated dots in an irradiated matrix (dose=1×10^{14} ions/cm^2), showing concentric perpendicular magnetic domains.

At a lower scale it is possible to analyze the domain structure of patterned samples (Fig. 12). The images have been acquired in the dc demagnetized state. The 1 μm-diameter nonirradiated dots in an irradiated matrix show a domain structure different from the continuous film, with concentric magnetic domains reflecting the shape of the dot, as theoretically predicted for laterally confined perpendicular structures.[41,42] On the other hand, the 250 nm dots appear as single domain structures (Fig. 13). The occurrence of bidomain state in symmetry broken systems is the analog of the vortex state. Such a phenomenology consists of two coaxial oppositely magnetized domains, of cylindrical symmetry, stable at zero-bias field. It depends on film thickness, dot radius, and intrinsic magnetic parameters (exchange length and anisotropy).[42] In order to compare properties of 1 μm-diameter dots with the corresponding physically isolated nanostructures we have also produced three-dimensional (3D) patterns of 1 μm dots by FIB milling with an ion dose of 2.6×10^{16} ions/cm^2.

The 1 μm-diameter milled dots do not show any evident domain structure (Fig. 14). This suggests that the cou-
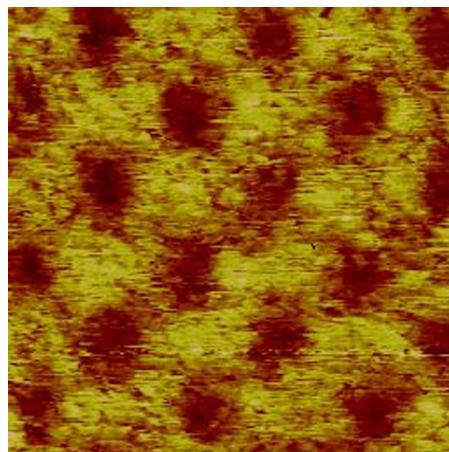
FIG. 13. (Color online) MFM image of the 2D patterned FePt films of 250 nm-diameter nonirradiated dots in an irradiated matrix (dose=1×10^{14} ions/cm^2).
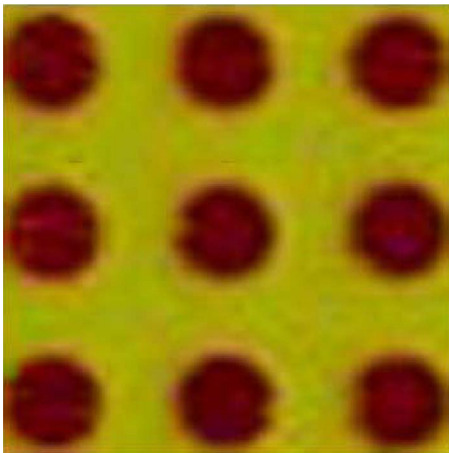
FIG. 14. (Color online) MFM image of the 3D patterned FePt films of 1 μm-diameter dots obtained by milling FePt films with a dose of 2.6 $\times 10^{16}$ ions/cm^2.

pling with the soft matrix influences the magnetic properties of the structures. The details of such couplings deserve further analysis.

IV. CONCLUSIONS

FePt perpendicular thin films of thickness $t=10$ nm were (001) epitaxially grown on MgO by RF sputtering and subsequently exposed to Ga$^+$ irradiation with ion beam energy of 30 keV. It was found that a Ga$^+$ dose of 1 $\times 10^{14}$ ions/cm^2 and above induce a complete transition from the ordered $L1_0$ to the disordered A1 phase, leading to a drastic decrease of the magnetic anisotropy and coercivity, and to a spin reorientation transition from out-of-plane to in-plane. At the same time, for low doses (up to 3×10^{15}) we found that the surface topography was not affected by ion irradiation.

Taking advantage of these results, 2D continuous patterns with controlled magnetization direction and coercivity were produced by locally modifying the film by FIB, using the lowest effective dose (1×10^{14} ions/cm^2). Arrays of $L1_0$ nonirradiated dots and stripes with perpendicular direction of magnetization in a soft A1 (irradiated) matrix with in-plane magnetization were obtained.

The 2D patterns were revealed by means of magnetic force microscopy. While no evident domain structure was observed in 250 nm dots, the 1 μm–diameter dots show a peculiar bidomain state with concentric magnetic domains that were found to be influenced by a coupling with the soft matrix.

[1] R. Skomski, A. Kashyap, and J. Zhou, Scr. Mater. **53**, 389 (2005).
[2] K. Barmak, J. Kim, L. H. Lewis, K. R. Coffey, M. F. Toney, A. J. Kellock, and J.-U. Thiele, J. Appl. Phys. **98**, 033904 (2005).
[3] F. Casoli, F. Albertini, S. Fabbrici, C. Bocchi, L. Nasi, R. Ciprian, and L. Pareti, IEEE Trans. Magn. **41**, 3877 (2005).
[4] G. Asti, M. Ghidini, R. Pellicelli, M. Solzi, F. Albertini, F. Casoli, S. Fabbrici, and L. Pareti, Phys. Rev. B **73**, 094406 (2006).
[5] E. Chunsheng, D. Smith, J. Wolfe, D. Weller, S. Khizroev, and D. Litvinov, J. Appl. Phys. **98**, 024505 (2005).
[6] S. Khizroev and D. Livitinov, *Perpendicular Magnetic Recording* (Kluwer, Boston, 2004), p. 129.
[7] A. Moser, C. Bonhote, Q. Dai, H. Do, B. Knogge, Y. Ikeda, Q. Le, B.

Lengsfield, S. MacDOnald, J. Li, V. Nayak, R. Payne, M. Schabes, N. Smith, K. Takano, C. Tsang, P. van der Heijden, W. Weresin, M. Williams, and M. Xiao, J. Magn. Magn. Mater. **303**, 271 (2006).
[8] H. J. Richter, J. Phys. D **40**, R149 (2007).
[9] D. E. Laughlin, S. Kumar, Y. Peng, and A. G. Roy, IEEE Trans. Magn. **41**, 719 (2005).
[10] Y. K. Takahashi, K. Hono, T. Shima, and K. Takanashi, J. Magn. Magn. Mater. **267**, 248 (2003).
[11] F. Casoli, F. Albertini, L. Pareti, S. Fabbrici, L. Nasi, C. Bocchi, and R. Ciprian, IEEE Trans. Magn. **41**, 3223 (2005).
[12] B. D. Terris and T. Thomson, J. Phys. D **38**, R199 (2005).
[13] B. S. H. Pang, Y. J. Chen, and S. H. Leong, Appl. Phys. Lett. **88**, 094103 (2006).
[14] C. Chappert, H. Bernas, J. Ferrè, V. Kottler, J. P. Janet, Y. Chen, E. Cambril, T. Devolder, F. Rousseaux, V. Mathet, and H. Launois, Science **280**, 1919 (1998).
[15] J. Fassbender, D. Ravelosona, and Y. Samson, J. Phys. D **37**, R179 (2004).
[16] J. P. Nozieres, M. Ghidini, N. M. Dempsey, B. Gervais, D. Givord, G. Suran, and J. M. D. Coey, Nucl. Instrum. Methods Phys. Res. B **146**, 250 (1998).
[17] S. Konings, J. Miguel, J. Luigjes, H. Schlatter, J. Luigjes, J. Goedkoop, and V. Gadgil, J. Appl. Phys. **98**, 054306 (2005).
[18] W. M. Kaminsky, G. A. C. Jones, N. K. Patel, W. E. Booij, M. G. Blamire, S. M. Gardiner, Y. B. Xu, and J. A. C. Bland, Appl. Phys. Lett. **78**, 1589 (2001).
[19] V. Parekh, D. Smith, E. Chunsheng, J. Rantschler, S. Khizroev, and D. Litvinov, J. Appl. Phys. **101**, 083904 (2007).
[20] Ch. Houpert, N. Nguyen, F. Studer, D. Groult, and M. Toulemonde, Nucl. Instrum. Methods Phys. Res. B **34**, 228 (1988).
[21] M. Cai, T. Veres, S. Roorda, R. W. Cochrane, R. Abdouche, and M. Sutton, J. Appl. Phys. **81**, 5200 (1997).
[22] D. Kurowski, R. Meckenstock, J. Pelzl, K. Brand, P. Sonntag, and P. Grünberg, J. Appl. Phys. **81**, 5243 (1997).
[23] C. Vieu, J. Gierak, H. Launois, T. Aign, P. Meyer, J. P. Jamet, J. Ferrè, C. Chappert, T. Devolder, V. Mathet, and H. Bernas, J. Appl. Phys. **91**, 3103 (2002).
[24] D. Ravelosona, C. Chappert, V. Mathet, and H. Bernas, Appl. Phys. Lett. **76**, 236 (2000).
[25] C. H. Lai, C. H. Yang, and C. C. Chiang, Appl. Phys. Lett. **83**, 4550 (2003).
[26] H. Bernas, J.-Ph-. Attanè, K.-H. Heinig, D. Halley, D. Ravelosona, A. Marty, P. Auric, C. Chappert, and Y. Samson, Phys. Rev. Lett. **91**, 077203 (2003).
[27] B. D. Terris, D. Weller, L. Folks, J. E. E. Baglin, A. J. Kellock, H. Rothuizen, and P. Vettiger, J. Appl. Phys. **87**, 7004 (2000).
[28] M. Abes, M. V. Rastei, J. Vénua, L. D. Buda-Prejbeanu, A. Carvalho, G. Schmerber, J. Arabski, E. Beaurepaire, J. P. Bucher, and A. Dinia, Mater. Sci. Eng., B **126**, 207 (2006).
[29] M. Abes, J. Venuat, D. Muller, A. Carvalho, G. Schmerber, E. Beaurepaire, A. Dinia, and V. Pierron-Bohnes, J. Appl. Phys. **96**, 7420 (2004).
[30] T. Hasegawa, G. Q. Li, W. Pei, H. Saito, S. Ishio, K. Taguchi, K. Yamakawa, N. Honda, K. Ouchi, T. Aoyama, and I. Sato, J. Appl. Phys. **99**, 053505 (2006).
[31] F. Casoli, L. Nasi, F. Albertini, S. Fabbrici, C. Bocchi, F. Germini, P. Luches, A. Rota, and S. Valeri, J. Appl. Phys. **103**, 043912 (2008).
[32] P. Vavassori, Appl. Phys. Lett. **77**, 1605 (2000).
[33] F. Casoli, F. Albertini, L. Nasi, S. Fabbrici, R. Cabassi, F. Bolzoni, and C. Bocchi, Appl. Phys. Lett. **92**, 142506 (2008).
[34] F. Albertini, L. Nasi, F. Casoli, S. Fabbrici, P. Luches, A. Rota, and S. Valeri, J. Magn. Magn. Mater. **316**, e158 (2007).
[35] S. Okamoto, N. Kikuchi, O. Kitakami, T. Miyazaki, Y. Shimada, and K. Fukamichi, Phys. Rev. B **66**, 024413 (2002).
[36] C. Kooy and U. Enz, Philips Res. Rep. **15**, 7 (1960).
[37] J. F. Ziegler, J. P. Biersack, and U. Littmark, *The Stopping and Range of Atoms in Solids* (Pergamon, New York, 1985).
[38] A. Cebollada, R. F. C. Farrow, and M. F. Toney, in *Magnetic Nanostructures*, edited by H. S. Nalwa (American Scientific, Stevenson Ranch, CA, 2002), pp. 93–121.
[39] ICSD database of the International Centre for Diffraction Data.
[40] S. Porthun, L. Abelman, and C. Lodder, J. Magn. Magn. Mater. **182**, 238 (1998).
[41] J. K. Ha, R. Hertel, and J. Kirshner, Europhys. Lett. **64**, 810 (2003).
[42] S. Komineas, C. A. F. Vaz, J. A. C. Bland, and N. Papanicolau, Phys. Rev. B **71**, 060405(R) (2005).